Multi-Packet Opportunistic Large Array Transmission on Strip-Shaped Cooperative Routes or Networks

Haejoon Jung, *Student Member, IEEE,* and Mary Ann Weitnauer*, *Senior Member, IEEE*

***Abstract*—The Opportunistic Large Array (OLA) is one type of cooperative transmission, which provides fast and reliable broadcasts and unicasts in multi-hop networks. While the existing literature on OLAs assumes one-shot transmission with a single packet, we analyze *multi*-packet OLA transmission within a single flow along strip-shaped networks or OLA-based cooperative routes. When multiple packets are transmitted from the same source using the same channel before the previous packet has cleared the network, which is called *spatial pipelining*, intra-flow interference is produced by OLAs transmitting co-channel packets. Using the continuum assumption (approximated by high density networks), the authors optimize the throughput. This paper theoretically shows spatial pipelining over strip networks is always feasible for path loss exponent $\alpha \geq 2$, which is not true for disk-shaped networks. Moreover, the impacts of system parameters are analyzed, and the upper bound of the optimal packet spacing (the lower bound of the optimal throughput) is derived. Also, spatial pipelining in finite networks is studied with numerical results, which confirm the theoretical analysis.**

***Index Terms*—Ad-hoc networks, cooperative diversity, transmit diversity.**

I. Introduction

CONCURRENT Cooperative transmission (CCT) is a physical layer technique, which combines multiple copies of the same message transmitted simultaneously by multiple, physically separated radios, and received over independently fading diversity channels. CCT provides a signal-to-noise ratio (SNR) advantage to the receiver through array and diversity gains [1]. One form of CCT is the Opportunistic Large Array (OLA), where groups of relays are formed without coordination by the relays' successful decoding of a message from a single node or another OLA [2]. The diversity channels can be formed using orthogonal waveforms [3], distributed space-time block codes [4], or phase dithering [5]. Practical OLA transmission has been demonstrated by the authors [6]. OLA-based broadcasts and unicasts are known to be fast, reliable, power-efficient and less susceptible to network partitions [7]. However, while most of these benefits are derived by the range extension property of CCT, one negative aspect of range extension is increased interference. For example, if multiple packets are transmitted using the same channel, each packet suffers from co-channel interference from the other packets propagating at the same time. In this paper, we investigate this "*intra-flow interference*" of the OLA transmission, which is generated by multiple OLAs transmitting different packets from the same source and heading for the same destination within a single flow.

There are three network models in the existing studies on OLA: 'disk', 'strip', and 'line' networks. While the disk networks model the multi-hop broadcasts in a large area by concentric rings as in [8] and [9], the strip networks characterize multi-hop unicasts using a cooperative route or muti-hop broadcasts using wireless nodes deployed in strip-shaped structures such as on roadways, bridges, and tunnels as in [10] and [11]. The disk and strip network models differ significantly in terms of the sizes and shapes of OLAs, as a function of hop number. For the single-shot (i.e., single-packet) transmission, the OLAs in the disk-shaped networks form concentric rings, and their areas generally grow exponentially with hop-count [8]. In contrast, the OLA step-sizes of the strip-shaped networks converge to a certain value, as the hop-count increases [10]. Different from the disk and strip networks, the research on line networks in [12] and [13] apply quasi-stationary Markov processes to study single-shot OLA transmission down an infinitely long line of nodes that can only exist in equally spaced positions [12], [13]. However, because of matrix size limitations, that work has not been extended to strip networks with width.

In this paper, we consider multi-packet OLA transmissions down a "strip" of finite width, such that the nodes are densely and randomly distributed over the strip. The primary motivation for studying this type of node distribution is that it is an idealization of a cooperative route through a large multi-hop network. Such a route can be formed many ways. It is the direct result of the route request (RREQ) and route reply (RREP) of the OLA-based protocols, OLAROAD [6], OLACRA [7], and CBR [14]. However, a strip-shaped route could also be formed using the set-up phase of a conventional shortest-path routing protocol, such as AODV [15], by defining the cooperative route as *all* the nodes that can *decode (or overhear)* the RREP message for a particular source-destination pair, or that can decode Hello messages sent by nodes on the

Manuscript received January 16, 2013; revised May 21 and August 29, 2013; accepted October 14, 2013. The associate editor coordinating the review of this paper and approving it for publication was M. Bhatnagar.

*Mary Ann Weitnauer was formerly Mary Ann Ingram.

The authors are with the Department of Electrical and Computer Engineering, Georgia Institute of Technology, Atlanta, GA, 30332 USA (e-mail: hjung35@gatech.edu, mary.ann.weitnauer@ece.gatech.edu).

The material in this paper was presented in part at the International Conference on Communications (ICC), June 2012, Ottawa, Canada.

The authors gratefully acknowledge partial support for this research from the National Science Foundation, grant number CNS-1017984.

Digital Object Identifier 10.1109/TWC.2013.112613.130093

primary (conventional) route. Or, the route can be formed geometrically assuming each node knows its geographical location (e.g., from GPS) [16]. Regardless of how the cooperative route is created, the Data-transmission phase can follow the method described in this paper, to achieve low latency and reliable packet transfer [6]. As stated earlier, there are also a number of applications for which the multi-hop network would just happen to have a strip-shape, such as vehicular networks on roadways or the structural health monitoring networks for bridges and tunnels [17]. One can also imagine a futuristic piece of plastic tape, with embedded radios on it, that could serve as a non-conducting "*communication cable*" [18].

This paper is focused on the throughput optimization of OLA transmissions down such a strip-shaped route or network, to support, for example, a transfer of a large file. For both disk- and strip-shaped networks, the system performance is evaluated in terms of the same metrics emphasized in the conventional non-CT multi-hop networks such as latency, energy-efficiency, and throughput. The end-to-end latency and the energy-efficiency of OLA technique are analyzed in [7]–[11]. However, these studies only consider the singe-shot (i.e., single-packet) scenario without the detailed consideration on the throughput, when multiple packets are transmitted. Compared to the single-shot latency analysis, the throughput optimization in the presence of the intra-flow interference by multiple co-channel packets is a more challenging problem, because the propagation behaviors of the multiple packets dynamically change by interactive influence on each other. This paper provides a guideline about how to determine the inter-packet spacing ultimately to optimize the throughput under the impact of various system parameters using analytical and numerical results.

To our knowledge, only one other group, Sirkeci-Mergen and Gastpar [19], considered multi-packet OLA broadcasting. However, [19] considered the "disk" network, in which the OLA size of a single packet can grow exponentially. Furthermore, [19] assumed perfect interference cancellation of interference from preceding packets, and analyzed the effects of the interference from the following packets. However, for some types of networks such as sensor networks, constraints on node processors and memory may preclude interference cancellation. Also, the presence of multiple time and frequency offsets of cooperators may make channel estimation very challenging [20]. Therefore, in contrast to [19], we assume that none of the interference is cancelled. Previously, we studied multi-packet co-channel broadcast transmission from the same source (referred to as spatial pipelining) in disk-shaped networks without the interference cancellation assumption, and found that OLA propagation behavior depends on the path loss exponent α [21], [22]. For $\alpha = 2$, the interference from the first packet is always high enough around the source to retard the area of the OLAs for the second packet, regardless of the inter-packet period. Consequently, for $\alpha = 2$, we found that spatial pipelining is not feasible for disk networks [21]. However, for $\alpha > 2$, we found spatial pipelining in disk networks is feasible and the packet insertion rate can be optimized [22]. This paper is distinguished from [19] by not assuming any interference cancellation. Moreover, different from [19], [21], [22], this paper analyzes the "strip" network, which can model unicast traffic transmitted by OLA.

The more confined geometry of the strip network gives different OLA propagation characteristics, compared to the disk. For example, for single-packet transmission and $\alpha = 2$, the OLA sizes approach a finite value with hop-count [10]. The conference version of this paper [23], which assumes $\alpha = 2$ and offers only numerical analysis, shows that spatial pipelining without any interference cancellation is feasible and can be optimized. To our knowledge, only [23] and this paper treat intra-flow interference in the strip-shaped network. This paper is distinguished from [23] by the following extensions. First, this paper generalizes the path loss exponent as $\alpha \geq 2$, while [23] only covers $\alpha = 2$. To be specific, as an initial but crucial step for the further discussion about the multi-packet scenario, we show the single-packet transmission behavior for $\alpha > 2$ in the strip network, which is not present in the existing literature. We believe this generalization of α is important, because α is a key factor that determines the optimal inter-packet spacing, as shown in the paper. Second, this paper explicitly shows a *stable* state in the multi-packet transmission dynamics, in which the multiple co-channel packets have almost equal hop-distance for a long period of time, while [23] only indirectly addresses its existence. Third, using the propagation behavior with this stable state, this paper theoretically proves the feasibility of the throughput optimization by spatial pipelining. Fourth, the impacts of the system parameters are investigated both theoretically and numerically (new numerical results with $\alpha = 2$, 3, and 4), while [23] only provides the numerical results with $\alpha = 2$.

The organization of the paper is as follows. In Section II, the system model using the continuum and deterministic channel assumptions is presented. Also, the concept of *spatial pipelining* is explained in detail, and the signal model of intra-flow interference is defined. In Section III, using example numerical results, we introduce the propagation characteristics of spatially pipelined OLA transmissions for the finite-length strip network. In Section IV, we explore the feasibility of spatial reuse by multiple co-channel OLAs in the infinite-length strip network with $\alpha \geq 2$. Moreover, the impacts of the system parameters on throughput are theoretically analyzed. In Section V, we optimize the throughput for the finite-length strip network and present an upper bound for the optimal packet insertion period for $\alpha \geq 2$. Section VI provides the numerical results about the optimal throughput and shows the relationships between the optimal throughput and the system parameters.

II. System Model

We consider a strip network with length of L and width of W, which is expressed by $\mathbb{S} = \{(x, y) : 0 \leq x \leq L, |y| \leq \frac{W}{2}\}$, where decode-and-forward (DF) wireless nodes are uniformly and randomly distributed with average density of ρ. Assuming unicast traffic, as shown in Fig. 1, the source node is at the origin, while the destination is at the right end separated by L from the source. The other nodes are operating DF relays that forward the packet only when the decoding is successful and the node has not transmitted the packet before [2]. On the other hand, since all nodes in our system

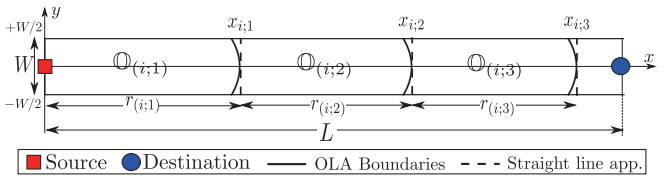

Fig. 1. The OLA transmission on the strip network based on the continuum assumption and straight line approximation.

model, besides the source, have the opportunity to receive the message, the results in this paper also apply to broadcasting.

As in [8] and [10], let P_s and P_r denote the power received by a node at unit distance from the source and relay, respectively. For simplicity, we assume the unit noise power, $\mathbf{N} = 1$. Thus, the received power can be used interchangeably with the received SNR. Assuming a path loss exponent of α, the path loss function is defined by $l(d) = 1/d^{\alpha}$, where d is the distance from the transmitter and the receiver. Therefore, when (x, y) is the location of a receiver relative to a transmitter in Cartesian coordinates, the SNR received from the source is $P_s \cdot l(d) = \frac{P_s}{(x^2+y^2)^{\alpha/2}}$. In the absence of interference, the decoding is assumed to be successful if the received SNR is greater than or equal to a certain threshold τ determined by the modulation and coding [8].

A. Deterministic Channel and Continuum Assumptions

For the multi-hop network analysis with a large number of nodes doing CT, we make the deterministic channel and continuum assumptions, as in [8]–[11] and [19], which allows simpler analysis, but is accurate enough for multi-hop OLA transmissions with high node density, as shown in [8] and [10]. In various studies on CT as in [24]–[26], multiple CT transmitters that are physically separated in space are approximated into a single node with multiple-antenna array, which is called *co-located approximation*. However, this co-located approximation causes a significant error especially for the high node density situation as shown in [27] and [28], because this model ignores the disparate path losses from the multiple transmitters to a receiver in a virtual multi-input-single-output (MISO) link of CT.

For this reason, following the "deterministic channel assumption" as in [8]–[11] and [19], we assume that each node in an OLA transmits in an orthogonal diversity channel and the power received at a node is the sum of the powers from each of the transmitting nodes. In other words, when a set of relays $\mathbb{O}$, in a network of finite node density, transmit together to a receiver, its received power can be calculated as $\sum_{j\in\mathbb{O}} P_r \cdot l(d_j)$. Also following [8]–[11], we make the "continuum assumption", which is verified as an accurate model for "finite but high" density networks as shown in [8]. In this continuum model focusing on the high density networks, the node density ρ goes to infinity, while the transmission power per unit area $\overline{P_r} = \rho P_r$ is held constant. We refer to this particular limit in the sequel as the *"continuum limit."* Because the nodes are uniformly distributed, each infinitesimal area has $\overline{P_r} dxdy$ transmit power by the continuum model. Therefore, the received power $\sum_{j\in\mathbb{O}} P_r \cdot l(d_j)$ can be approximated into an integral form as $\iint_{\mathbb{O}} \overline{P_r} \cdot l(d) dA$, where A is the area of $\mathbb{O}$.

Since the "sum of powers" property is based on the assumption of every relay transmitting in an orthogonal diversity channel, and in the limit of the continuum, the number of relays goes to infinity, we seem to be assuming infinite bandwidth. However, in practice, only a finite number of orthogonal diversity channels are used, and if these channels are allocated uniformly, then the number of channels is the diversity order. Furthermore, as the diversity order grows, the increase in diversity gain diminishes [29], corresponding to an effective reduction in fading in the SNR after combining. Therefore, our assumptions apply to networks with high node densities and a high number of diversity channels. For example, the authors in [7] show that packet delivery ratio (PDR) of the flat fading channel with a finite node density ($\rho = 2.2$) gets closer to the results based on the "sum of powers" property with the deterministic channel assumption, as they increase the number of diversity channels from one to four. Similarly, in [30], the simulation results of the probability of successful broadcast (PSB) that assumes uniformly and randomly distributed nodes with $\rho = 10$ in Rayleigh fading channel show an excellent match with the analysis based on the deterministic channel assumption, as the number of diversity channels increases from one to three.

It follows from a finite number of diversity channels, that one could assign orthogonal channels for consecutive packets (i.e., simultaneously using different OLAs), which would eliminate the intra-flow interference. However, similarly to the diversity channel allocation to the multiple nodes in an OLA, the number of the channels assigned to the multiple OLAs would be limited in practice. Therefore, if a large file were being broadcasted over a large multi-hop network, channels may need to be reused, in which case, the results in this paper would still apply.

In further support of our system model based on the continuum and deterministic channel assumptions, we note that the simulation results in [7], [10] and the theoretical study in [8] show that the system with cooperative orthogonal transmission has a deterministic SNR by continuum assumption even in the presence of fading and randomness in the channel, which ultimately gives the same result based on the deterministic channel assumption. Therefore, we note that the theoretical and numerical approaches in this paper still work for random fading channels with finite but high node density as well.

B. Validity in Finite-density Networks

In this section, the applicability and limitation of the analytical model based on the two assumptions are described. This paper is focused on how multiple packets propagate in space, the analysis of which is facilitated by the deterministic channel and continuum assumptions. To be specific, we are mainly interested in *packet loss* in multi-packet OLA transmission, which means a packet does not reach the edge of a multi-hop network, for a given inter-packet separation. In the continuum limit, packet loss is indicated in terms of number of hops; that is, a packet is lost if it stops propagating within a finite number of hops (i.e., OLA levels), which is referred to as *transmission die-off* in [8] and [10]. On the other hand, in a real OLA network with finite node density, where the number

and placement of nodes are random, packet loss occurs when there is no node that successfully decodes the packet at an intermediate hop before reaching the network edge.

The simulation results in [10], which assume the strip-shaped network, show the propagation prediction based on the continuum assumption is accurate for high enough node density, specifically $\rho = 30$, 50, and 100. For example, when $\rho = 30$, the prediction error in OLA propagation (boundary) is less than 2% compared to the simulation results. Moreover, in their disk-shaped network study in [8], the continuum analysis shows less than 5% error of the spatial propagation of OLAs to the simulation results of random and finite-density disk networks, when $\rho = 10$ and 100.

On the other hand, the continuum analysis is not accurate for low node density networks corresponding to $\rho \leq 5$, as shown in the simulation results in [10] and [8]. To be specific, the propagation speed becomes highly random with high standard deviation, as ρ decreases. In particular, for low node-density networks with random fading channel, the packet propagates significantly faster in some parts of the network, while slower in other areas by the opportunistic feature of OLA, which is inflated by random node placement. However, we note that because of analytical difficulty to predict this highly random propagation characteristic, this paper is focused on the high node density network with $\rho \geq 10$, where the analysis based on the deterministic channel and continuum assumptions is accurate to model the real network with uniform and random node placement.

C. Single-Packet OLA Transmission

With these assumptions, the first level OLA for the ith packet is the area denoted by $\mathbb{O}_{(i;1)}$, as shown in Fig. 1, with boundary $x_{(i;1)}$ that satisfies $P_s/x_{(i;1)}^{\alpha} = \tau$. Also, for Level $k \geq 1$, the nodes that have not transmitted the packet (Packet i) so far will join the next level $k+1$, if their received SNR, the signal component of which is determined by the received power from the current level OLA $\mathbb{O}_{(i;k)}$, is greater than or equal to τ. In other words, subsequent OLAs $\mathbb{O}_{(i;k)}$ of this packet without interference for $k \geq 2$ are formed by the SNR condition, which is given by

$$\mathbb{O}_{(i;k)} = \{(x,y) \in \mathbb{S} \setminus \bigcup_{n=1}^{k-1} \mathbb{O}_{(i;n)} : \iint_{\mathbb{O}_{(i;k-1)}} \frac{\overline{P_r}}{[(x-x')^2 + (y-y')^2]^{\alpha/2}} dx'dy' \leq \tau\}. \quad (1)$$

As shown in [10], when the width W is small enough, the curved boundaries of the OLAs can be approximated by straight lines indicated by the dashed lines in Fig. 1. Therefore, the approximated OLA, $\tilde{\mathbb{O}}_{(i;k)}$, is the area that satisfies $x_{(i;k-1)} \leq x \leq x_{(i;k)}$ and $|y| \leq \frac{W}{2}$. Suppose the location of a receiver is $(z,0)$ such that $z < x_{(i;k-1)}$ or $z > x_{(i;k)}$ at the time that OLA $\tilde{\mathbb{O}}_{(i;k)}$ is transmitting. The SNR at this receiver is denoted as

$$P(\tilde{\mathbb{O}}_{(i;k)} \to z) = \iint_{\tilde{\mathbb{O}}_{(i;k)}} \frac{\overline{P_r}}{[(x-z)^2 + y^2]^{\alpha/2}} dxdy = \int_{-W/2}^{W/2} \int_{x_{(i,k-1)}}^{x_{(i,k)}} \frac{\overline{P_r}}{[(x-z)^2 + y^2]^{\alpha/2}} dxdy, \quad (2)$$

where the OLA level index $k = 1, 2, 3, ...$, and $x_0 = 0$. Therefore, the outer boundary of $(k+1)$st OLA, $x_{(i;k+1)}$ is the solution of $P(\tilde{\mathbb{O}}_{(i;k)} \to z) = \tau$ such that $z > x_{(i;k)}$. Let $r_{(i;k)} = x_{(i;k)} - x_{(i;k-1)}$ be the step-size of ith packet for kth level. We treat this integral equation differently, depending on if the path loss exponent α satisfies $\alpha = 2$ or $\alpha > 2$, because the analytical methods are different.

In spite of the different analytical methods, the two following subsections will show that, for any $\alpha \geq 2$, the single-packet OLA propagation with large enough $\overline{P}_r$ reaches the steady-state, in which the step-size $r_{(i;k)}$ converges to a fixed value, as the OLA level index k increases. In other words, the sizes (i.e., hop-distances) of OLAs of a single packet are kept to be the same after a certain k. We point out that the second case with $\alpha > 2$ is not present in the existing literature.

1) Free Space Path Attenuation ($\alpha = 2$): For $\alpha = 2$, the received power equation in (2) can be expressed by

$$P(\tilde{\mathbb{O}}_{(i;k)} \to z)|_{\alpha=2} = \int_{x_{(i,k-1)}}^{x_{(i,k)}} \frac{2\overline{P_r}}{(x-z)} \arctan\left(\frac{W}{2(x-z)}\right) dx, \quad (3)$$

The behavior of the single-shot (i.e., single-packet) OLA transmission is well studied in [10], when $\alpha = 2$. They derive the sufficient condition for the propagation to the infinite-length strip network, in the absence of interference; the condition is $\mu < 2$, where $\mu = \exp(\frac{\tau}{\pi \overline{P_r}})$.

This condition is interpreted with a physical meaning in [7] using *node degree* $\kappa = \frac{\rho P_r}{\tau}$, which means the average number of nodes in the decoding range of a node as we will now explain. The decoding range of a relay is given by the area inside the circle around the relay with the radius of r_{siso}, where $\frac{P_r}{r_{siso}^{\alpha}} = \tau$. Therefore, in a finite-density network with density ρ, the node degree κ is given by

$$\kappa = \rho \pi r_{siso}^2 = \rho \left(\frac{P_r}{\tau}\right)^{2/\alpha}. \quad (4)$$

We observe that when $\alpha = 2$, the node degree is constant in the continuum limit, because $\overline{P}_r = \rho P_r$ is constant as $\rho \to \infty$ and $P_r \to 0$. Thus, the condition for $\alpha = 2$ is $\kappa > (\ln 2)^{-1}$. In other words, the node degree, which is proportional to the transmit power P_r and node density ρ, should be large enough for the sustained single-packet OLA transmission. When this condition holds, as the OLA level goes to infinity, the step-size converges to a positive number $r_{(i,\infty)}$, which satisfies $\frac{W(\pi \ln 2 - \overline{P_r}/\tau)}{4} \leq r_{(i;\infty)} \leq \frac{W\overline{P_r}}{2\tau}$ [10].

2) Higher Path Attenuation ($\alpha > 2$): Many indoor and short-range wireless networks are lossy with higher path loss exponents, so we also investigate the OLA propagation with higher path loss exponent $\alpha > 2$, which is not covered in [10]. Following the analytical approach in [10] for $\alpha = 2$, to show the steady-state with equal step-size, we will first derive the relationship between the step-sizes of two consecutive OLA levels, k and $k+1$, by defining a function $r_{(i;k+1)} = h\left(r_{(i;k)}\right)$. Then, we will prove the existence of the steady-state satisfying $r_{(i;k+1)} = r_{(i;k)}$ that corresponds to the solution of $x = h(x)$ by showing the properties of $h(\cdot)$.

First, when $\alpha > 2$, the received power in (2) is given by

$$P(\tilde{\mathbb{O}}_{(i;k)} \to z)|_{\alpha>2} = \int_{x_{(i;k-1)}}^{x_{(i;k)}} \frac{\overline{P}_r \left(\frac{W^2}{4} + (x-z)^2\right)^{-\alpha/2} \left(W^2 + 4(x-z)^2\right)}{4W(\alpha-2)(x-z)^2} \times \left[\left(W^2 + 4(x-z)^2\right) {}_2F_1\left(1, \frac{3-\alpha}{2}, \frac{-1}{2}, \frac{-W^2}{4(x-z)^2}\right) + \left((\alpha-5)W^2 - 4(x-z)^2\right) {}_2F_1\left(1, \frac{3-\alpha}{2}, \frac{1}{2}, \frac{-W^2}{4(x-z)^2}\right) \right] dx, \quad (5)$$

where $k = 1, 2, 3, ...$, $x_0 = 0$, and ${}_2F_1(\cdot,\cdot,\cdot,\cdot)$ is the Gauss Hypergeometric function [31]. As the previous case with $\alpha = 2$, to find the next OLA boundary $x_{i;k+1}$, we need to solve the equation $P(\tilde{\mathbb{O}}_{(i;k)} \to z) = \tau$, which can be expressed in terms of the step-size $r_{(i;k+1)}$ because $x_{(i;k+1)} = x_{(i;k)} + r_{(i;k+1)}$. By the variable change with $u = (x - z)$, this equation can be expressed as

$$\int_{r_{(i;k+1)}}^{r_{(i;k+1)}+r_{(i;k)}} \frac{\left(\frac{W^2}{4} + u^2\right)^{-\alpha/2} \left(W^2 + 4u^2\right)}{4W(\alpha-2)u^2} \times \left[\left(W^2 + 4u^2\right) {}_2F_1\left(1, \frac{3-\alpha}{2}, \frac{-1}{2}, \frac{-W^2}{4u^2}\right) + \left((\alpha-5)W^2 - 4u^2\right) {}_2F_1\left(1, \frac{3-\alpha}{2}, \frac{1}{2}, \frac{-W^2}{4u^2}\right) \right] du = \frac{\tau}{\overline{P}_r}. \quad (6)$$

Let $G(u, \alpha, W)$ be the term inside the integral. Then, the subsequent step-sizes can be iteratively obtained with $r_{(i;k+1)} = h\left(r_{(i;k)}\right)$, where the function $h\left(r_{(i;k)}\right)$ is defined as the unique solution of $\int_{h\left(r_{(i;k)}\right)}^{h\left(r_{(i;k)}\right)+r_{(i;k)}} G(u, \alpha, W)du = \tau/\overline{P}_r$ for $r_{(i;k)} > 0$. The following properties for $h(\cdot)$ are proved in the Appendix.

1) For any $x > 0$, there exists a unique solution, $h(x)$, for $\int_{h(x)}^{h(x)+x} G(u, \alpha, W)du = \frac{\tau}{\overline{P}_r}$. By continuity $h(0) := \lim_{x\to 0} h(x) = 0$.
2) The function $h(\cdot)$ is monotonically increasing.
3) The function $h(\cdot)$ is concave.

Fig. 2 displays these properties of $h(x)$, where the black straight line displays $y = x$ graph, and the red (curved) solid line and the dashed line indicate $h(x)$ curves of $\alpha = 2$ and 3, respectively. The three properties proven here for $\alpha > 2$ are identical to the findings about $h(x)$ when $\alpha = 2$ in [10]. Therefore, as proven in [10], if $h(x) = x$ has a solution except $x = 0$, which corresponds to the crossing points of $y = h(x)$ and $y = x$ curves in Fig. 2, the OLA propagation reaches the steady-state with OLA step-size converged to the solution (i.e., $r_{(i;\infty)} = x$). For example, the black dotted line indicates how the one-shot OLA transmission reaches the steady-state with $\alpha = 2$. Because of more severe path attenuation, the limiting step-size decreases as α increases as indicated by the crossing points of Fig. 2. While $h'(0)$ has a closed form expression for $\alpha = 2$, which corresponds to the sufficient condition for sustained single-packet OLA transmission in a strip network (i.e., $\mu < 2$ for $\alpha = 2$) as shown in [10], it is very difficult to obtain the closed form expression of $h'(0)$, when $\alpha > 2$. As a result, it is also difficult to derive the sufficient condition for sustained single-packet OLA transmission along the strip network in a closed form for $\alpha > 2$. However, by the analytical properties for $\alpha > 2$ proved in the Appendix, we can conclude that the propagation patterns for the both cases ($\alpha = 2$ and $\alpha > 2$) reach a steady-state with high enough relay transmission power $\overline{P}_r$. Furthermore, in constant to $\alpha = 2$, for $\alpha > 2$, there is no notion of κ in the continuum limit. We observe that the exponents of ρ and P_r in (4) are different, and therefore, κ is not constant as the continuum limit is approached for $\alpha > 2$.

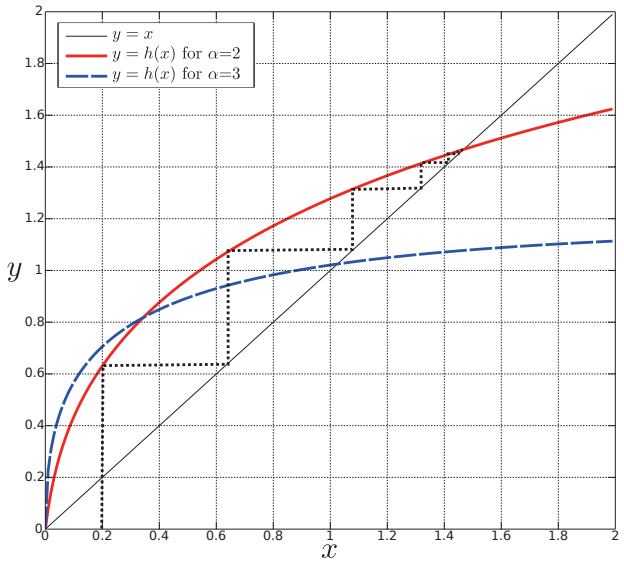

Fig. 2. $h(x)$ curves for $\alpha = 2$ and 3, when $\overline{P}_r = 3$, $\tau = 1$, and $W = 1$.

D. Signal Model of Intra-flow Interference

We consider multiple packets transmitted from the source to the destination, with no interference from any other flows in the network. Instead, we only consider "intra-flow" interference with in a single flow. We use the definition of the throughput in [32]: the rate at which packets cross a measurement boundary. In some applications, such as large file transfer, throughput is more important than end-to-end latency of a single packet. If the boundary is at the origin where the source is located, the throughput is identical to the reciprocal of the packet insertion period of the source (i.e., how often the source can send a new data packet into the network). In the conventional network with single-input-single-output (SISO) links, the source inserts a new packet when the channel around the source is available again after the last packet, because carrier sense multiple access with collision avoidance (CSMA/CA) is used [33]. However, we note that CSMA/CA, which results in nodes initiating transmission at random times, is not desirable for the OLA transmission, because of the autonomous and distributed control in each node and the need for synchronized transmission. The transmit time synchronization for the same OLA can be achieved based on Global Positioning System (GPS) [5]. Also, in the

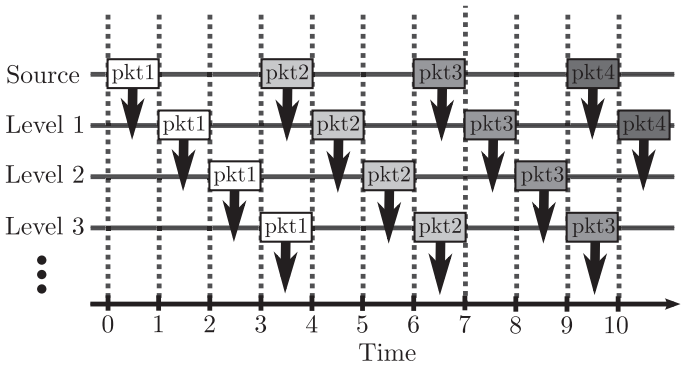

Fig. 3. Timing diagram of spatial pipelined OLA with $M = 3$.

absence of GPS or other external devices, the preamble-based transmit time synchronization method developed in our research group can be used, as demonstrated using a software-defined radio (SDR) platform in indoor environments in [34]." To be specific, the transmit time synchronization scheme in [34] is designed to support the OLA transmissions. In this scheme, the relays doing CT use embedded time stamp, which is based on the reception from the previous hop, to hold the packet for a fixed period before firing. The experimental results in [34] show the mean rms transmit time spreads on the order of $50ns$ in indoor environments.

We define one time unit is the time duration required for transmission and reception over one hop. Suppose n is the total number of packets to be sent with a packet insertion period M (i.e., the source sends a new data packet into the network every M time units). We are interested in the network throughput, which is equal to $\eta = 1/M$ for large enough n. Fig. 3 shows an example of spatially pipelined OLA transmissions with $M = 3$, where the horizontal axis indicates time, while the vertical axis indicates OLA level. As shown in the figure, the source inserts a new packet (from Packet 1 to 4) with a fixed period $M = 3$, and the following level OLAs also forward the packets periodically. Therefore, multiple packets, indicated by the squares with different brightness, are propagating across the network at the same time using the same channel with certain inter-separations, which is called *spatial pipelining*.

For simplicity to explain the signal model, suppose only two packets are transmitted: the second packet is transmitted by the source M time units after the first packet transmission. Fig. 4 shows a part of a long strip network with the length of L and width of W. The shaded areas in Fig. 4 indicate two OLAs that could be transmitting at the same time. Suppose the smaller one, $\tilde{\mathbb{O}}_{(2;k)}$, transmits the second packet in its $k+1$st hop, and $\tilde{\mathbb{O}}_{(1;k+M)}$, transmits the first packet in its $k+M+1$st hop. We are interested to know if receivers at Points A at $(x_A, 0)$ and B at $(x_B, 0)$ will be able to decode Packets 1 and 2, respectively. We note that $x_{(1;k+M)} < x_A$ and $x_{(2;k)} < x_B < x_{(1;k+M-1)}$.

For the receiver at Point A, we have,

$$\mathbf{SINR}_{(1;k+M+1)}(x_A) = \frac{\mathbf{S}}{\mathbf{I}+\mathbf{N}} = \frac{P(\tilde{\mathbb{O}}_{(1;k+M)} \to x_A)}{P(\tilde{\mathbb{O}}_{(2;k)} \to x_A) + 1}. \tag{7}$$

We will assume that if this SINR is greater than τ, the receiver can decode. For the receiver at Point B, the interference comes

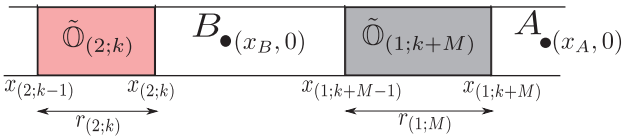

Fig. 4. The snapshot of multiple-packet OLA broadcast.

from $\tilde{\mathbb{O}}_{(1;k+M)}$, which is to the right of Point B. Thus, for the receiver at Point B, the SINR is

$$\mathbf{SINR}_{(2;k+1)}(x_B) = \frac{P(\tilde{\mathbb{O}}_{(2;k)} \to x_B)}{P\left(\tilde{\mathbb{O}}_{(1;k+M)} \to x_B\right) + 1}. \tag{8}$$

Therefore, $x_A = x_{(1;k+M+1)}$ satisfies $\mathbf{SINR}_{(1;k+M+1)}(x_A) = \tau$, while $x_B = x_{(2;k+1)}$ satisfies $\mathbf{SINR}_{(2;k+1)}(x_B) = \tau$.

III. Multi-packet Propagation for the Finite Strip

In this section, we explore the properties in multi-packet OLA propagations along a strip network of finite length, using numerical analysis. The results motivate the theoretical approach for the infinite strip case in the following section.

As an example to show the impact of the co-channel interference, we numerically calculate the propagation dynamics with $\alpha = 2$, $P_s = 100$, $\overline{P_r} = 100$, $\tau = 10$, $W = 1$, and $L = 200$. Even though $\alpha = 2$ is used in this example, we note that the following properties in this section are common for any $\alpha \geq 2$. If the source sends only one packet, there is no intra-flow interference. For the given parameters, a single packet takes 41 hops for the single packet to reach the destination by OLA transmission, which we denote by $M_0 = 41$. Therefore, with a fixed packet insertion period M, if the source injects new packets, interference will occur if $M < M_0 = 40$; we refer to this situation as *spatial pipelining*.

Fig. 5 shows the numerical results of the OLA transmission with ten packets for $M = 10$, where the x-axis indicates time, and the y-axis denotes the propagation distance in terms of the horizontal distance from the source ($x_{(i;k)}$ in Fig. 1). The ten black solid curves represent the OLA propagations of the ten packets as time evolves, while the red dashed lines are the reference curves showing the interference-free (or the single-packet OLA transmission) situation that we denote by $x_{(0;k)}$. The numbers with the bold font on the black curves indicate the final hop-counts when the packets finish propagations. Also, the slopes of the black curves in the figure mean the step-sizes $r_{(i;k)} = x_{(i;k)} - x_{(i;k-1)}$, while the slope of the red curve indicates the interference-free step-sizes $r_{(0;k)} = x_{(0;k)} - x_{(0;k-1)}$. Fig. 6 shows the numerical results of a shorter packet insertion period of $M = 5$, where we observe that Packets 3, 6, and 8 are lost, because they quit propagating.

A. Upper Bounds on Hop-Counts and Step-sizes

Because of the co-channel interference, the step-sizes of the pipelined OLA transmission are smaller than the step-sizes of the single-packet OLA transmission, where co-channel interference does not exist. In Figs. 5 and 6, the step-size decrease causes the slope of the black curves to be lower than the red

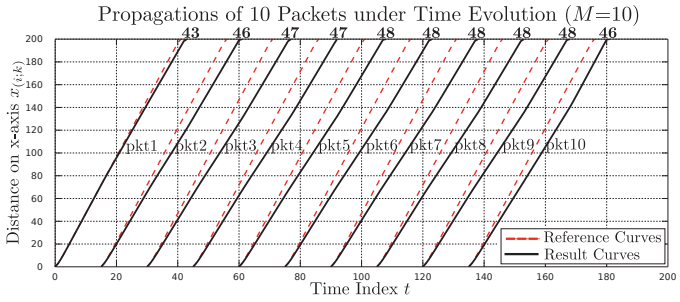

Fig. 5. The time evolution of the hop distances, when $M = 10$.

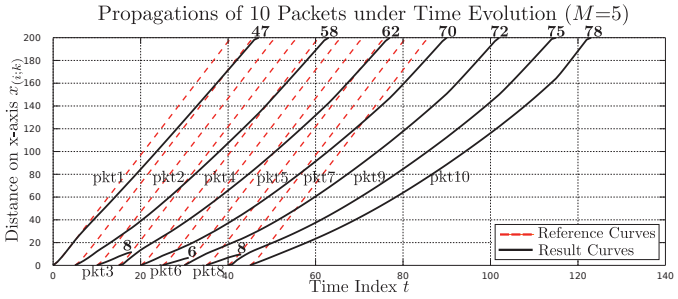

Fig. 6. The time evolution of the hop distances, when $M = 5$.

dashed curves. Also, because $x_{(i;k)}$ is the accumulated value of the step-sizes, it is bounded by $x_{(0;k)}$. Therefore, regardless of the packet insertion period, $r_{(i;k)} \leq r_{(0;k)}$ and $x_{(i;k)} \leq x_{(0;k)}$ always hold. This property is important to estimate the range of the OLA boundaries, which is required to numerically calculate the SINR equation. Because $x_{(i;k)} \leq x_{(0;k)}$ always holds, the final hop-counts of the packets in Figs. 5 and 6 are greater than $M_0 = 40$ except the packet loss cases in Fig. 6.

B. Packet Insertion Period

If the final hop-count at the destination for the single-packet case is M_0, the range of the packet insertion period M for the spatial pipelining is $3 \leq M \leq M_0 - 1$, assuming a half-duplex system. In this range, the intra-flow interference increases as M decreases, because a smaller M means the shorter inter-packet distances. However, if M is too small, some packets die off in the middle of the network as do Packets 3, 6, and 8 in Fig. 6, because the inter-packet spacing is not enough to keep the SINR above the decoding threshold τ. As indicated by the decreasing slopes of Packets 3, 6, and 8, the step-sizes $r_{(i;k)}$ of the three packets gradually decrease as hop goes. Since the received power is proportional to the area of the transmitting (i.e., current-hop) OLA, the smaller step-size of the current hop makes the step-size of the next hop even smaller. At the same time, as the step-sizes of Packets 3, 6, and 8 decrease, the SINRs of their neighboring co-channel packets (Packets 2, 4, 5, 7, and 9) increase, since the interferences from Packet 3, 6, 8 become smaller. For this reason, the three packets finally stop propagating right after the time when their OLA sizes become too small to exceed the decoding threshold. Because this packet loss results in a waste of time and energy, which reduces the throughput, it is significant to choose the appropriate M to maximize the network throughput without causing any packet loss. Also, while Fig. 6 shows the time-varying slopes, the slope of each packet curve in Fig. 5 is almost stable, because the step-size change between adjacent hops is very small.

C. Worst-Case Packet

Depending on the packet index, packets have different propagation patterns in terms of the hop distance and hop-count. As long as no packets are lost, the first packet always shows the fastest propagation, because it does not experience interference until the second packet comes into the network. For a similar reason, the first and last few packets undergo relatively less interference, because the numbers of their co-channel packets are smaller compared to the packets with the intermediate indices. For example, in Fig. 5, among the ten packets, Packet 1 shows the smallest final hop-count of 43, and its slope in Fig. 5 is also the highest. Packets 2 and 10 also show the relatively smaller hop-counts of 46, while Packet 5 to 9 have 48. If looking at the curve of Packet 5 in Fig. 5, the instantaneous slope is minimized around when $x_{(5;k)} \approx 100$, which is the horizontal mid-point of the strip network. Suppose there are three consecutive co-channel packets along a strip network as a simplified example. Among the three packets, the one in the middle always has the highest total interference. In conclusion, if no packets are lost, a packet experiences the highest interference, when it is the middle one of the sequence (i.e., $i \approx 50$, if the total number of packets is 100), and when it is in the middle of the strip (i.e., $x_{(i;k)} \approx L/2$).

D. Stable State with Equal Step-size

For multiple-packet OLA transmission in the finite-length strip networks, the steady-state of the single-packet propagation is perturbed, when a new following packet is inserted or a preceding packet reaches the destination. In this situation, there are two kinds of perturbation factors in terms of the packet index and the location in the network. To be specific, for a large enough network length L and a large number of packets n, the first and last few packets show the different propagation patterns from the packets with the intermediate indices, because the network is not fully filled with multiple co-channel packets when the first and last few packets propagate. Also, the packets with the intermediate indices reach a *stable state* with an almost equal step-size in the middle area of the network (the neighborhood of the network mid-point: $x_{(i;k)} \approx L/2$), where the packets are less affected by the new insertion of the following packets and the exit of the preceding packets at the both ends.

As an example, Fig. 7 shows the step-sizes of multiple packets with the horizontal axis of the OLA level index k and the vertical axis of the step-sizes $r_{(i;k)}$, which are numerically computed with 200 packets. The other parameters are identical to Fig. 5 (i.e., $\alpha = 2$, $P_s = 100$, $\overline{P_r} = 100$, $\tau = 10$, $W = 1$, $L = 200$, and $M = 10$). In the figure, the first 40 and last 40 packets, which have the packet indices $1 \leq i \leq 40$ and $161 \leq i \leq 200$, are indicated by the black dotted lines, while the intermediate 120 packets, which have the indicated $41 \leq i \leq 160$, are indicated by the red solid lines. All the 200 packets (both the black dotted line and red solid lines) show the flat bowl-shaped curves, excluding the sudden drops of

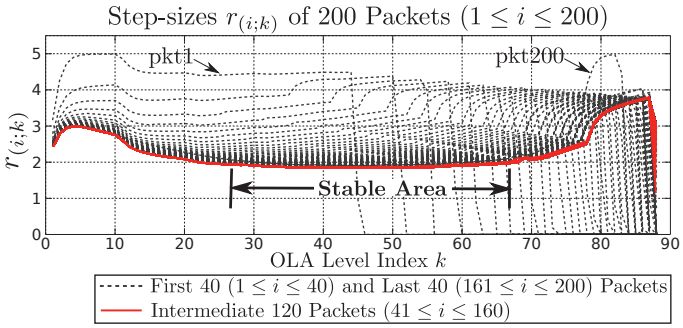

Fig. 7. The overlapped step-sizes $r_{(i;k)}$ curves of 200 packets.

the final step-size clipped by the network edge, because the numbers of the neighboring co-channel packets are smaller around the both ends as explained in the previous section, which makes the propagation speed faster around the network boundaries than the propagation speed in the middle area of the strip.

However, the overlapped curves of the 200 packets are quite different in terms of the total hop-counts and the fluctuation levels, which are indicated by the widths and heights, respectively. On the other hand, the red solid curves representing the 120 packets with the intermediate indices ($41 \le i \le 160$) show almost the same pattern, if excluding the black dotted curves indicating the packets that experience a partially filled network (i.e., $1 \le i \le 40$ and $161 \le i \le 200$). Also, the middle area of the overlapped red curves has relatively stable heights, where $r_{(i;k)}$ does not change significantly for different OLA level index k, because it is physically far from the both ends and less affected by the perturbations from the network boundaries (i.e., $x_{(i;k)} \approx 0$ or L). This observation is the motivation for our analytical approach in the next section. If both the number of packets n and the network length L go to infinity, the throughput performance should be governed by this stable state with a fixed step-size propagation.

This stable state can be found by observing the step-sizes of consecutive packets. Numerically, we can start searching from the mid-sequence packet $i' = N/2$, by picking its OLA level k', the boundary of which is closest to the mid-point of the network (i.e., $x_{(i';k')} \approx L/2$. Then, the stable state range in terms of the OLA level, which is denoted by $k_{min} \le k \le k_{max}$, for the same packet i' can be defined by the indices k that have almost equal step-sizes $|r_{(i';k)} - r_{(i';k')}| < \epsilon$ with a certain $\epsilon \approx 0$ (e.g., $0.01 \cdot r_{(0;k')}$, where $r_{(0;k')}$ is the interference-free step-size). After that, the stable state range across different packets can be found by searching the packet indices i that satisfy $|r_{(i;k)} - r_{(i';k)}| < \epsilon$ for the same $k_{min} \le k \le k_{max}$.

IV. Spatial Pipelining in the Infinite Strip Network

In this section, we consider the spatially pipelined OLA transmission for the infinite-length strip network in presence of co-channel interference from the preceding and following packet OLAs. The "infinite" network is a theoretical concept, but it provides an intuition to explain the multi-packet OLA transmission in a large network, where a large number of hops are required for a packet to reach the destination.

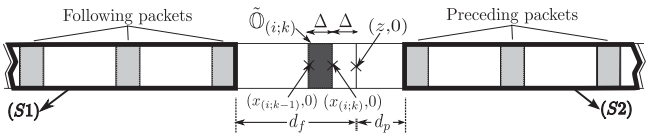

Fig. 8. Illustration of the spatially pipelined OLA transmission in infinite strip network.

A. Feasibility of Spatial Pipelining

If the spatial pipelining in the infinite network is feasible, there should be a finite packet insertion period M that does not cause packet loss for infinitely many packets on the fly. This feasibility issue can be proved by showing that the simultaneously transmitted co-channel packets are at-least-linearly propagating down the strip. The core idea used in the proof (at-least-linearly propagating OLAs) is the same as [19], which proves the feasibility in the *disk-shaped network* with *interference cancellation* from the preceding packets. In the following, we extend this result to strip networks and no cancellation.

Theorem 1: For finite τ that is small enough compared to the transmission powers $\overline{P_r}$ and P_s, an infinite number of the spatially pipelined packets are feasible to propagate at least linearly with a fixed step-size Δ for a finite packet insertion period of M, without causing packet loss in the infinite-length strip network.

Proof: We focus on the worst-case scenario in Section III-C assuming the infinite length, where a packet is in between infinitely many preceding and following co-channel packets as shown in Fig. 8. If this packet (the dark-gray one in Fig. 8) propagates at least linearly with a fixed step-size Δ, then the other packets (the light-gray ones in Fig. 8) also propagate at least linearly. We inflate the co-channel interference by treating all the inter-packet separation areas between any consecutive interfering OLAs as interfering areas, which makes two (preceding and following) infinitely large interfering OLAs: the two areas $(S1)$ and $(S2)$ indicated by the thick black lines in Fig. 8. We will prove that if the worst-case packet has the inter-separation of $M\Delta$ to the two infinitely-large-area interfering OLAs, this packet is at-least-linearly propagating by Δ.

Suppose the packets are inserted with the period of M. In Fig. 8, the dark-gray area is the desired signal source $\tilde{\mathbb{O}}_{(i;k)}$, while the light-gray areas represent the interfering OLAs $\tilde{\mathbb{O}}_{(i+j;k-Mj)}$ with $j \neq 0$, which are infinitely many for infinite L. For Packet i to propagate at least linearly, its kth level boundary $x_{(i;k)}$ must satisfy

$$x_{(i;k)} \ge k\Delta, \tag{9}$$

where Δ is an arbitrary positive number. Moreover, the kth step-size $r_{(i;k)}$ of $\tilde{\mathbb{O}}_{(i;k)}$ must satisfy $r_{(i;k)} \ge \Delta$. To satisfy (9), the received SINR at Point z, which is Δ away from $x_{(i;k)}$, should be greater than or equal to τ. For the SINR calculation in this proof, we use the two large OLAs $(S1)$ and $(S2)$ in

Fig. 8. First, the received signal power $\mathbf{S}$ at Point z has an lower bound $\mathbf{S}_{LB}$, which is derived as

$$\begin{aligned}\mathbf{S} &= P(\tilde{\mathbb{O}}_{(i;k)} \to z) \\ &> \frac{\overline{P}_r \cdot Area[\tilde{\mathbb{O}}_{(i;k)}]}{(2\Delta)^\alpha} = \frac{\overline{P}_r W}{2^\alpha \Delta^{\alpha-1}} = \mathbf{S}_{LB}, \quad (10)\end{aligned}$$

where $\alpha \geq 2$ and $W < \Delta$ for the rectangular approximation in Fig. 1. On the other hand, the interference is divided into two: the interferences from the preceding packets and from the following packets, which are denote by $\mathbf{I}_p$ and $\mathbf{I}_f$, respectively. Using the "two infinite-length OLAs" approach, the separation from Point z to $(S1)$ is d_f, while the separation from Point z to $(S2)$ is d_p. When the packets propagate at least linearly, $d_f \geq (M+1)\Delta$ and $d_p \geq (M-2)\Delta$. Hence, the upper bound for the interference $\mathbf{I}_{UB}$ with packet insertion period of M can be given by

$$\begin{aligned}\mathbf{I} &= \sum_{j\neq 0} P(\tilde{\mathbb{O}}_{(i+j;k-Mj)} \to z) = \mathbf{I}_p + \mathbf{I}_f \\ &< \overline{P}_r W \int_{(M-2)\Delta}^{\infty} \frac{1}{x^\alpha} dx + \overline{P}_r W \int_{(M+1)\Delta}^{\infty} \frac{1}{x^\alpha} dx \\ &= \frac{\overline{P}_r W}{(\alpha-1)\Delta^{\alpha-1}} \left(\frac{1}{(M-2)^{\alpha-1}} + \frac{1}{(M+1)^{\alpha-1}} \right) \\ &< \frac{2\overline{P}_r W}{(\alpha-1)\Delta^{\alpha-1}(M-2)^{\alpha-1}} = \mathbf{I}_{UB}, \quad (11)\end{aligned}$$

Therefore, using (10) and (11), we can derive the lower bound of the received SINR at Point z, which is denoted by $\mathbf{SINR}_{LB}$. Therefore, the co-channel packets propagate at least linearly, if the following inequality holds to satisfy the decoding condition at Point z:

$$\mathbf{SINR}_{LB} = \frac{\mathbf{S}_{LB}}{\mathbf{I}_{UB}+1} = \frac{\frac{\overline{P}_r W}{2^\alpha \Delta^{\alpha-1}}}{\frac{2\overline{P}_r W}{(\alpha-1)\Delta^{\alpha-1}(M-2)^{\alpha-1}}+1} \geq \tau. \quad (12)$$

Because $\mathbf{SINR}_{LB}$ is a monotonically increasing function of M, when $\tau < \infty$ with large enough $\overline{P}_r$, there always exists a solution pair (M, Δ), where $M \geq 3$ and $\Delta > 0$. Therefore, if kth level OLA has a step-size of Δ, the $(k+1)$st level OLA also has a step-size greater than or equal to Δ with a finite M.

Also, when a new packet is inserted at the source, which corresponds to $k = 0$, the signal component $\mathbf{S}$ of P_s/Δ^α, and the interference is only from the preceding packets because it does not have any following packet yet. Therefore, the interference from the preceding packets, which is smaller than $\mathbf{I}_{UB}$ in (11), is a monotonically decreasing function of M. Hence, with large enough P_s, we can guarantee the initial step-size $r_{(i;1)} = \Delta$ by using a finite M as well. Thus, it is shown that (9) can be satisfied with finite M as long as the decoding threshold is also finite. ∎

B. Lower Bound of Optimal Throughput for the Interference-limited Case

The most important issue in the pipelined OLA transmission is the selection of M; we want the smallest value of M that causes no packet loss, so the throughput $\eta = 1/M$ is maximized. Suppose $M_{I,opt}$ is the minimum packet insertion period M for given parameters such as α, $\overline{P}_r$, τ, and W, with which the spatially pipelined OLA transmission with infinitely many co-channel packets is sustained in the infinite network. Then, if $\hat{M}_{I,opt}$ is the minimum M that satisfies the inequality in (12), $M_{I,opt} \leq \hat{M}_{I,opt}$ always holds, and the corresponding throughputs satisfy $\eta_{I,opt} \geq \hat{\eta}_{I,opt}$. Therefore, we can find the lower bound of the throughput $\hat{\eta}_{I,opt} = 1/\hat{M}_{I,opt}$ using (12).

However, it is difficult to solve (12), because there are too many variables. The number of variables can be reduced by letting $\overline{P}_r \to \infty$, where the interference is significantly greater than the noise power. In the limit, $\mathbf{SINR}_{LB}$ in (12) becomes

$$\mathbf{SIR}_{LB} = \frac{\mathbf{S}_{LB}}{\mathbf{I}_{UB}} = \frac{(\alpha-1)(M-2)^{\alpha-1}}{2^{\alpha-1}}. \quad (13)$$

If we solve $\mathbf{SIR}_{LB} \geq \tau$, it gives the minimum packet insertion period as

$$\hat{M}^*_{I,opt} = \left\lceil 2\left(\frac{\tau}{\alpha-1}\right)^{\frac{1}{\alpha-1}} \right\rceil + 2, \quad (14)$$

where the ceiling is because $\hat{M}^*_{I,opt}$ is a positive integer, which is a function of just two parameters: α and τ.

1) $\hat{M}^*_{I,opt}$ and α: In the single-shot (or single-packet) transmission, the higher path loss exponent α degrades the propagation speed of the packet, but for the multiple-packet transmission with spatial pipelining, the higher α can be beneficial, because the spatial reuse becomes more efficient as α grows. The following corollary proves the improvement of throughput resulted by the better spatial reuse with higher α.

Corollary 1: For the interference-limited case, the lower bound of the throughput $\hat{\eta}^*_{I,opt}$, which is equal to $1/\hat{M}^*_{I,opt}$, increases as α increases for $1 < \alpha \leq 1+e^\tau$ when the decoding threshold τ is fixed.

Proof: For simplicity, excluding the ceiling on the right hand side in (14), we define a function $q(\alpha) = 2\left(\frac{\tau}{\alpha-1}\right)^{\frac{1}{\alpha-1}} + 2$, which is less than or equal to the original term with the ceiling. If we differentiate $q(\alpha)$ with respect to α, we have $q'(\alpha) = \frac{\partial q}{\partial \alpha}$ as

$$q' = -2\left[\frac{\ln\left(\frac{\tau}{\alpha-1}\right)+1}{(-1+\alpha)^2}\right]\left(\frac{\tau}{\alpha-1}\right)^{\frac{1}{\alpha-1}}, \quad (15)$$

where the solution of $q'(\alpha) = 0$ is $1+e^\tau$. The second derivative $q''(\alpha) = \frac{\partial^2 q}{\partial \alpha^2}$ to test the concavity is given by

$$q'' = 2\left(\frac{\tau}{\alpha-1}\right)^{\frac{1}{\alpha-1}}\left[\frac{3+2\ln\left(\frac{\tau}{\alpha-1}\right)}{(\alpha-1)^3} + \frac{\left(1+\ln\left(\frac{\tau}{\alpha-1}\right)\right)^2}{(\alpha-1)^4}\right]. \quad (16)$$

Because $q''(\alpha = 1+e^\tau) = 2\cdot\exp(-3-\frac{1}{e^\tau})/\tau^3$ is always positive, the function $q(\alpha)$ is minimized at $\alpha^* = 1+e^\tau$. Moreover, because $q'(\alpha) < 0$ when $1 < \alpha < \alpha^*$, $q(\alpha)$ decreases as α increases. With the ceiling as in (14), $\hat{M}^*_{I,opt}$ decreases or stays the same, as α increases. Hence, in this range, the lower bound of the throughput $\hat{\eta}^*_{I,opt}$ increases, as α increases. ∎

As a practical example, we assume $\tau > 1$, which corresponds to the class of bandwidth-efficient waveforms for large file transfer [35]. Specifically, $\alpha^* \approx 3.718$ for $\tau = 1$, and $\alpha^* \approx 8.389$ for $\tau = 2$. Therefore, in the practical ranges of τ and α, the lower bound of the throughput $\hat{\eta}^*_{I,opt}$ increases, as α increases, which confirms the better spatial reuse for higher α.

2) $\hat{M}^*_{I,opt}$ and τ: The decoding threshold τ is a important parameter that determines the required inter-packet separation, the increase of which makes the throughput decrease, for the sustained OLA transmission with multiple packets. The following corollary shows the impact of τ on the lower bound of the throughput $\hat{\eta}^*_{I,opt}$ for the interference-limited case.

Corollary 2: For the interference-limited case with $\overline{P}_r \to \infty$, the lower bound of the throughput $\hat{\eta}^*_{I,opt}$ decreases as τ increases.

Proof: We must show $\hat{M}^*_{I,opt}$ increases when τ increases. Hence, if we differentiate q, which is defined in Corollary 1, with respect to τ, we have $\frac{\partial q}{\partial \tau}$ as

$$\frac{\partial q}{\partial \tau} = \frac{2\left(\frac{\tau}{\alpha-1}\right)^{\frac{2-\alpha}{\alpha-1}}}{(\alpha-1)^2}, \tag{17}$$

which is always positive, when $\tau > 0$ and $\alpha > 1$. Therefore, q is a increasing function of τ. Hence, $\hat{M}^*_{I,opt}$, which is equal to ceiling of q, increases or stays the same (by the ceiling), as τ increases. ∎

We note that while the increase in τ reduces the packet insertion rate at the source, the network capacity and transmission rate, which is defined as $R = \log_2(1+\tau)$ in [19], increases, when τ increases. For example, when τ increases, we can use higher-order modulation or increase the packet size. However, we limit our scope to the packet-level analysis (i.e., how often we can insert the packet at the source) following [32].

The two corollaries can be applied to the finite network with large enough L, where a large number of hops are required to reach the edge of the network, as long as the interference is significantly greater compared to the unit noise power. In the numerical results with the finite networks in Section VI, we observe the identical trends of the throughput depending on α and τ.

V. Optimal Packet Insertion Period in the Finite Network

In this section, we investigate the throughput optimization for finite strip networks that has a finite length L. However, we still focus on large enough length L, where the final hop-count of the single-packet OLA transmission, M_0, is large. Otherwise, it is a trivial problem, and there is not a significant advantage of the spatial pipelining compared to the simple OLA transmission with $M = M_0$ (no-spatial pipelining).

Finding the optimal packet insertion period $M_{L,opt}$ (the minimum M that does not cause packet loss for finite L) requires numerical calculation of the OLA boundaries $x_{(i;k)}$ for the all packet indices i and levels k at each time unit. Also, this numerical calculation should be repeated for different M starting from 3, to see whether there is packet loss. To limit this exhaustive search of $M_{L,opt}$, we might use $\hat{M}_{I,opt}$ in Section IV, which corresponds to the lower bound of the throughput in the infinite network. However, the interference term in $\hat{M}_{I,opt}$ is so highly inflated by integrating the infinitely many co-channel OLAs that $\hat{M}_{I,opt}$ actually makes an excessively loose upper bound in the finite strip case. Therefore, we propose a new upper bound of $M_{L,opt}$ assuming $\alpha = 2$, which give an appropriate range for the exhaustive search by *equal step-size* approximation based on the observations in Section III. This upper bound is derived using the sustained single-packet OLA transmission condition in [10] for the free space path loss ($\alpha = 2$). Moreover, because $M_{L,opt|\alpha=2} \geq M_{L,opt|\alpha>2}$ by the increased spatial reuse efficiency with higher α, the upper bound of $M_{L,opt}$ with $\alpha = 2$ is also the upper bound for the general case $\alpha \geq 2$.

A. Equal Step-size Approximation

To guarantee the sustained spatial pipelining without packet loss, we need to focus on the worst-case scenario: the packet with index i in the middle sequence and $x_{(i;k)} \approx L/2$ according to third observation in Section III, and keep it alive. Also, if L is large enough, the co-channel OLAs have almost the equal step-size over the wide area around the mid-point of the network, which is shown in the fourth observation in Section III. For this reason, we approximate the multi-packet OLA propagation patterns with the equal step-size to find the upper bound for $M_{L,opt}$. By assuming equal step-size, we neglect the "*edge effect*" in the finite network, or equivalently, we examine an L-long window of the infinite strip.

B. Upper Bound of $M_{L,opt}$ with $\alpha = 2$

Under the equal step-size assumption, the condition for an infinite OLA propagation is the same as that for a single isolated packet (i.e., $\mu < 2$ as in Section II), with unity noise power replaced by noise-normalized interference power plus one:

$$\exp\left[\frac{\tau(1+\mathbf{I})}{\pi\overline{P}_r}\right] < 2, \tag{18}$$

where $\mathbf{I} = \sum_{j\neq 0} P\left(\tilde{\mathbb{O}}_{(i+j;k-jM)} \to x_{(i;k+1)}\right)$ and the step-size of $\tilde{\mathbb{O}}_{(i+j;k-jM)}$ is Δ. A solution pair (M,Δ) must satisfy (18) as well as the step-width condition:

$$\mathbf{SINR}_{(i;k+1)}(z) = \frac{P(\tilde{\mathbb{O}}_{(i;k)} \to z)}{\mathbf{I}+1} = \tau, \tag{19}$$

where $z = x_{(i;k+1)} = x_{(i;k)} + \Delta$ for all i and $|x_{(i;k)} - x_{(j;k)}| = M\Delta|i-j|$ for all k. For given M and Δ, the maximum number of packets pipelined in the network is $n = \lceil \frac{L}{M\Delta} \rceil$. Hence, for Packet i in the middle, the number of its preceding co-channel packets is $n_p = \lceil \frac{n-1}{2} \rceil$, while the number of its following packets is $n_f = \lfloor \frac{n-1}{2} \rfloor$. Therefore, when $(n-1)$ is odd, $n_p = n_f + 1$, which is because we consider the worst-case scenario and $n_p = n_f + 1$ gives higher interference than $n_f = n_p + 1$, considering the propagation direction. Thus, with the number of co-channel packets n_p and n_f, we are able to test if the given Δ and M satisfy (18) and (19). If $\hat{M}_{L,opt}$ is the minimum M that satisfies these two conditions, $\hat{M}_{L,opt} > M_{L,opt}$.

C. Possible Multi-packet Transmission Strategy

We can consider a simple algorithm to find the optimal packet insertion period $M_{L,opt}$ that maximizes the throughput by using $\hat{M}_{L,opt}$ as the upper bound of $M_{L,opt}$, when the system parameters are known. To find $M_{L,opt}$, the source first needs to know the hop count M_0 from the source to the destination, where the destination is located. Because the theoretical bound $\hat{M}_{L,opt}$ in this section is obtained by assuming the free space path loss ($\alpha = 2$), $M_{L,opt} \leq \hat{M}_{L,opt}$ for $\alpha > 2$. Therefore, in general case with $\alpha \geq 2$, the search range of $M_{L,opt}$ is $3 \leq M \leq \min(M_0, \hat{M}_{L,opt})$.

The end-to-end hop count M_0 in the absence of the co-channel interference can be identified in the routing process. As stated in Section I, the strip network models a cooperative route between a source and destination pair formed by on-demand routing protocols such as such as OLAROAD [6], OLACRA [7], and CBR [14]. These OLA-based routing schemes require two end-to-end handshakes from the source to the destination as demonstrated in [6]: first handshake is to build a route using route request (RREQ) and route reply (RREP) and second handshake to check the route is valid using two additional control packets, route confirm (RC) and route confirm acknowledgement (RCACK). If RC, which is sent from the source to the destination in the second handshake, has the same data rate and packet length (by adding dummy bytes at the end of RC) as the data packet to have the same transmission ranges, RC will have the same hop-count characteristics as the data transmission in a static channel. Therefore, the destination can identify M_0, when it receives the RC originated from the source, because the RC has a hop count field incremented by one in each hop. After the destination receives the RC, it sends the RCACK, which contains the end-to-end hop count M_0 information, back to the source. Therefore, when the source receives the RCACK, it can obtain M_0 and use this information to limit the search scope of $M_{L,opt}$.

The search method of $M_{L,opt}$ for $3 \leq M \leq \min(M_0, \hat{M}_{L,opt})$ can be different (e.g., increasing, decreasing, or tree-based search) depending on the system requirements or applications. Regardless of the searching method, the packet loss before reaching the edge (i.e., destination) caused by $M < M_{L,opt}$ can be detected in various ways. First, the error can be detected at the source through end-to-end error control in OLA-based unicasts. As suggested in [36] and [14], end-to-end error recovery, which is similar to the end-to-end error control in the Transmission Control Protocol (TCP), is more desirable in OLA-based unicasts compared to link-layer error control, because of random OLA levels and possible link asymmetry between two consecutive OLAs that have different numbers of cooperators [37]. Therefore, using the end-to-end feedback such as acknowledgement (ACK) signal sent from the destination using an orthogonal control channel, the source can detect the packet loss occurred with $M < M_{L,opt}$.

Alternatively, the packet loss can be found in intermediate OLAs by the virtual ACK as in [7], which is simply the OLA transmission that the current level OLA overhears from the next level OLA in the next time slot (i.e., right after the transmission of the current level OLA). To be specific, in the multi-hop OLA transmission, Level k OLA forwards the packet received from Level $(k-1)$ OLA. Therefore, the nodes in Level $(k-1)$ OLA will detect an error (or packet loss) of their transmission to Level k OLA, if they cannot hear the data forwarding from Level k to Level $(k+1)$ for a fixed time duration in the following time slot, which implies Level k OLA fails to received the packet from Level $(k-1)$ OLA. If the packet loss is detected by Level $(k-1)$ OLA by this virtual ACK, the nodes in Level k OLA will send a feedback signal (i.e., negative acknowledgement (NACK)) to the source. Then, the source can detect the error and adapt the packet insertion period M to be longer. We note that the design of any link-level ACK or NACK scheme using OLAs is very challenging and outside the scope of this paper.

Once the optimal packet insertion period $M_{L,opt}$ is found in a finite-length strip network with given system parameters such as $\overline{P}_r$, τ, α, we can expect how $M_{L,opt}$ will change under the variation of a single parameter from the initial set-up based on the theoretical results in Section IV and the numerical results in the next section. However, we note that more detailed protocol design to find $M_{L,opt}$ and its evaluation are outside the scope of this paper.

VI. Numerical Analysis of Optimal Throughput in the Finite Strip Network

In this section, we present three sets of numerical results for optimal throughput using spatially pipelined OLA transmission in the finite network. The optimal packet insertion period $M_{L,opt}$ in the following results are obtained by exhaustive search, which corresponds to the optimal throughput $\eta_{L,opt} = 1/M_{L,opt}$ for an infinite number of packets. We test a finite number of packets (but large enough to fill the network fully pipelined) for the numerical computation.

The following numerical results show the effects of different system parameters such as $\overline{P}_r$, τ, and α on $M_{L,opt}$. However, because the distance between the packets or the OLA step-sizes can be an arbitrarily small positive number, the path loss function simply defined by $l(d) = 1/d^{\alpha}$ does not hold for very small d [38]. Therefore, as in [8], [10], for the numerical evaluations in this paper, we separate the path loss function depending on d to avoid unrealistically inflated received power, which is given by

$$l(d) \triangleq \begin{cases} 1/d^{\alpha}, & d \geq 1, \\ 1, & d < 1. \end{cases}, \tag{20}$$

where d is the normalized distance by d_0.

A. Impact of P_s, $\overline{P}_r$, and α on $M_{L,opt}$ with $\alpha = 2$, 3, and 4

We first look at the effect of the transmit powers P_s and $\overline{P}_r$ on the optimal packet insertion period $M_{L,opt}$, which is obtained by exhaustive search with given α. By comparing the three cases with different α, we will also consider the impact of α. In the numerical results in Fig. 9, we observe the variation in $M_{L,opt}$, which is indicated by the y-axis, when P_s and $\overline{P}_r$, which are indicated by the x-axis, increase from 5×10^4 to 10^5 with 10^4 intervals. We use 50 packets with $\tau = 10^3$ and $W = 1$. Moreover, to measure the degree of the throughput improvement by the ratio $M_{L,opt}/M_0$, we set

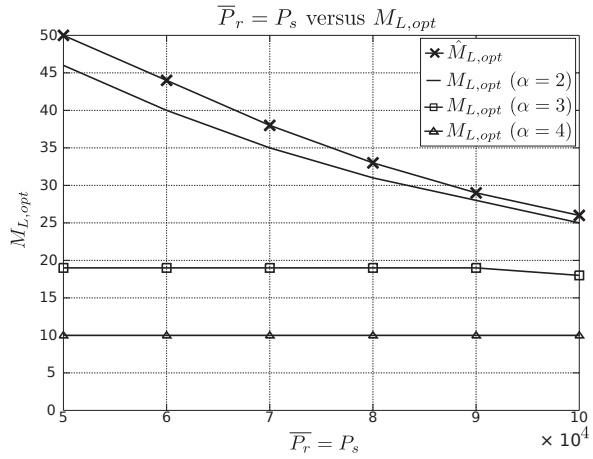

Fig. 9. Numerical results with the increasing $\overline{P}_r$=P_s, when $\tau = 10^3$, $W = 1$ and $L = 1200, 215, 121$ for $\alpha = 2, 3, 4$, respectively.

TABLE I
AVERAGE STEP-SIZES OF PACKET 25 WITH DIFFERENT TRANSMIT POWERS

	$P_s = \overline{P}_r$					
α	5×10^4	6×10^4	7×10^4	8×10^4	9×10^4	10×10^4
2	20.101	27.272	32.432	36.363	40.231	44.444
3	2.172	2.471	2.756	3.071	3.413	2.722
4	1.407	1.476	1.571	1.642	1.691	1.754

the different lengths $L = 1200$, 215, and 121 for $\alpha = 2$, 3, and 4, respectively, to have the same final hop-count for the single-packet OLA transmission as $M_0 = 50$ with the same $P_s = \overline{P}_r = 5 \times 10^4$. Therefore, the smaller $M_{L,opt}$ means more efficient spatial pipelining compared to $M_0 = 50$, because the throughput increases as M decreases.

In the figure, the curve with the 'x'-markers indicates the upper bound $\hat{M}_{L,opt}$ derived in Section V. Also, the solid line with no marker represents $M_{L,opt}$ found by exhaustive search with $\alpha = 2$, while $\alpha = 3$ and 4 cases are indicated by the curves with the square and triangle markers, respectively. If comparing the four curves at the same transmit powers $P_s = \overline{P}_r$, $\hat{M}_{L,opt} > M_{L,opt}$ always holds for all α. Also, the higher path loss exponent α gives lower $M_{L,opt}$, which means that we can expect more throughput improvement by spatial pipelining with higher α, which is consistent with Corollary 1 in Section IV.

The upper bound $\hat{M}_{L,opt}$ and the optimal $M_{L,opt}$ with $\alpha = 2$ show sharp decreases, as P_s and $\overline{P}_r$ increase, because the increase in the signal power $\mathbf{S}$ is relatively bigger than the increase in the interference $\mathbf{I}$ by the physical distances. In other words, the increase in $\overline{P}_r$ improves SIR at the desired receiver. Also, because $\overline{P}_r$ increases, while τ is fixed, SINR increases, because noise becomes insignificant. For the same reasons, smaller M (i.e., shorter inter-packet spacing) can be accommodated. As a result, $M_{L,opt}$ decreases, as the transmit powers increase. On the other hand, the optimal packet insertion periods $M_{L,opt}$ with $\alpha = 3$ and 4 are less sensitive to the transmit power change compared to $\hat{M}_{L,opt}$ and $M_{L,opt}$ with $\alpha = 2$. In the figure, $M_{L,opt}$ with $\alpha = 3$, which is represented by the solid line with square markers, decreases only by one at $P_s = \overline{P}_r = 10^5$, while $M_{L,opt}$ with $\alpha = 4$, which is indicated by the solid line with the triangle markers, does not change. That is simply because the impacts of the transmit powers on $M_{L,opt}$ with higher exponents ($\alpha = 2$ and 3) are not large enough, because of the high attenuation. In other words, the increases in P_s and $\overline{P}_r$ should be more significant for the higher path loss exponent cases to reduce $M_{L,opt}$ considerably.

Even though $M_{L,opt}$ does not change much with $\alpha = 3$ and 4, the increase of SINR can be noticed by the variation of the step-size. Table I shows the step-sizes, which are averaged over all OLA levels, of the middle sequence packet (Packet 25) that experiences the lowest SINR as explained in Section III-C. In the table, the three rows correspond to $\alpha = 2$, 3, and 4, while the columns indicate the six transmit power levels. As the transmit powers increase, the average step-sizes also increase for all cases except only when $P_s = \overline{P}_r = 10^5$ and $\alpha = 3$. This exception is because $M_{L,opt}$ decreases by one at the corresponding point. At this point, the improvement of SINR by increasing transmit powers is enough to accommodate the reduction of $M_{L,opt}$ for $\alpha = 3$. On the other hand, for $\alpha = 2$, both the reduction of $M_{L,opt}$ in Fig. 9 and the growth of the step-size in Table I happen at the same time. That is because the significant step-size growth with $\alpha = 2$ reduces the number of co-channel packets in the network significantly, which again inflates the SINR and the step-size. In contrast, the higher path loss exponents cases with $\alpha = 3$ and 4 show relatively slower increases of step-size than $\alpha = 2$, which does not significantly reduce the number of co-channel packets in the network.

B. Impact of τ and α on $M_{L,opt}$ with $\alpha = 2$, 3, and 4

The second set of numerical results in Fig. 10 present the impact of the decoding threshold τ on the optimal packet insertion period $M_{L,opt}$ for different path loss exponents $\alpha = 2$, 3, and 4, with 50 packets, $W = 1$, and $P_s = \overline{P}_r = 5000$. As shown in the figure, the x-axis indicates the decoding threshold $\tau = 25$, 50, 75, and 100, while the y-axis represents $M_{L,opt}$. Also, the optimal packet insertion periods $M_{L,opt}$ are found by exhaustive search with 50 packets, choosing different lengths L to keep the same final hop-count for the single-packet OLA transmission $M_0 = 50$ for different τ. Moreover, as in Fig. 9, the graph with the 'x'-markers indicates the upper bound $\hat{M}_{L,opt}$, while the other three graphs, which correspond to the different path loss exponents $\alpha = 2$, 3, and 4, are indicated by the solid lines with no markers, the square markers, and the triangle markers, respectively.

In the figure, all the four curves increase, as τ increases, which means the optimal inter-packet spacing increases. This behavior is identical to Corollary 2 in Section IV. Also, when comparing the heights of the three curves indicating $M_{L,opt}$ at the same τ, a curve with the lower path loss exponent has the greater $M_{L,opt}$ than the higher path loss exponent curve(s). Furthermore, among the three curves representing $M_{L,opt}$, the slopes of the $\alpha = 2$ graph is the highest, compared to the curves with $\alpha = 3$, and 4, which means that the '$\alpha = 2$' case is the most sensitive to the increase in τ. For $\alpha = 3$ and 4, because the slopes of the two $M_{L,opt}$ curves are close to zero, the corresponding throughputs $1/M_{L,opt}$ slightly decrease. The decoding threshold τ depends on other various parameters

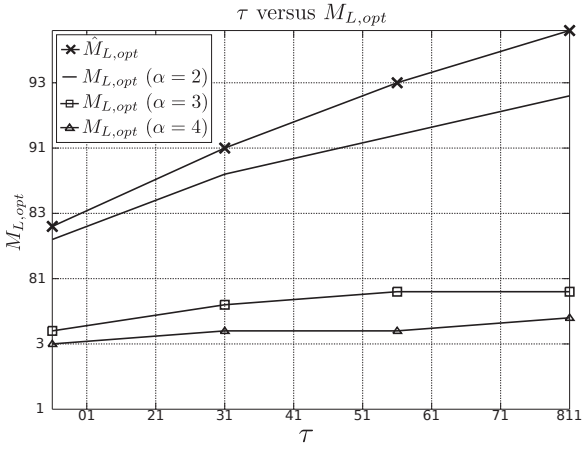

Fig. 10. Numerical results with the increasing $\tau = 25, 50, 75, 100$ for path loss exponents $\alpha = 2, 3, 4$, when $P_s = \overline{P_r} = 5000$, $M_0 = 50$, and $W = 1$.

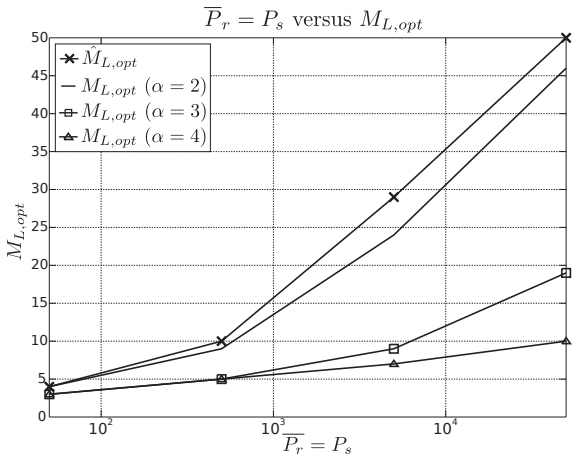

Fig. 11. Numerical results for the same ratio of $\frac{\overline{P_r}}{\tau}$: ($P_s$,$\overline{P_r}$,$\tau$)=(50,50,1), ($5\times10^2$,$5\times10^2$,10), ($5 \times 10^3$,$5 \times 10^3$,$10^2$), ($5 \times 10^4$,$5 \times 10^4$,$10^3$), when $\alpha = 2, 3, 4$, $M_0 = 50$, and $W = 1$.

(e.g., modulation order, packet size, and coding scheme) that change the data rate with non-trivial relationships. In this study, we limit our scope to the packet-level analysis with the assumption that the parameters deciding τ is fixed for a certain system.

Moreover, the graph corresponding to the upper bound $\hat{M}_{L,opt}$ is always higher than the three other curves representing $M_{L,opt}$ with $\alpha = 2$, 3, and 4, which implies that the upper bound is applicable for any $\alpha \geq 2$. Moreover, if comparing the heights of the three curves of $M_{L,opt}$ corresponding to $\alpha = 2$, 3, and 4, at the same x values, we can find $M_{L,opt}$ decreases as α increases. In other words, as the path loss exponent α increases, the throughput improvement by spatial pipelining becomes more significant, which confirms Corollary 1 in Section IV.

C. Impact of Simultaneous Variations in $\overline{P_r}$ and τ with Fixed Ratio for $\alpha = 2$, 3, and 4

In the last set of numerical results, we explore the impact of simultaneous variations in $\overline{P_r}$ and τ, when the ratio of the two is fixed. Also, we explore the impact of α by comparing the results with $\alpha = 2$, 3, and 4. Fig. 11 shows how the optimal packet insertion period $M_{L,opt}$ varies over different path loss exponents $\alpha = 2$, 3, and 4 with 50 packets, $W = 1$, and the fixed ratio of $\frac{\overline{P_r}}{\tau} = 50$. Based on (4), $\kappa = 50\pi$, when $\alpha = 2$, while κ is not defined in the continuum limit with $\alpha > 2$ as discussed at the end of Section II-C2. We consider four different sets of parameters as (P_s,$\overline{P_r}$,τ) = (50,50,1), (5×10^2,5×10^2,10), (5×10^3,5×10^3,10^2) and (5×10^4,5×10^4,10^3), where $\frac{\overline{P_r}}{\tau} = 50$. Moreover, as in the previous numerical results, we set the different lengths $L = 1200$, 215, and 121 for $\alpha = 2$, 3, and 4, respectively, to see the throughput enhancement by the ratio $M_{L.opt}/M_0$ for the same $M_0 = 50$, when the ratio $\frac{\overline{P_r}}{\tau}$ is held constant.

In the resulting figure, Fig. 11, the x-axis indicates $P_s = \overline{P_r}$ in log scale, and the y-axis represents $M_{L,opt}$ in linear scale with the same legend as in Figs. 9 and 10. First, all the four curves increase, as the parameter sets move from the first: (50,50,1), to the last: (5×10^4,5×10^4,10^3). By increasing transmit powers P_s and $\overline{P}_r$, the received SINR increases as shown in the previous numerical results in Fig. 9 and Table I. Therefore, with a fixed τ, smaller inter-packet spacing would be possible as shown in the previous results. At the same time, however, by the increase of τ, SINR requirement becomes more demanding, which exceeds the influence of the increase in $\overline{P_r}$. Thus, the simultaneous increases of transmit powers and τ, while keeping the same ratio of the two, result in the increase of $M_{L,opt}$. Moreover, in the graph, $M_{L,opt} \leq \hat{M}_{L,opt}$ always holds, which verifies the upper bound. As the previous results, the upper bound curve indicating $\hat{M}_{L,opt}$ is always higher than $M_{L,opt}$ for all $\alpha = 2$, 3, and 4, which verifies the upper bound. Moreover, as the previous numerical results and Corollary 1 in Section IV, the optimal packet insertion period $M_{L,opt}$ decreases, as α increases.

VII. Conclusion

In this paper, we analyze the impact of the intra-flow interference in the multi-packet OLA transmission over the strip networks using the continuum and deterministic channel assumptions, which pertain to the high density networks. We present the signal model and the properties of the spatially pipelined OLA transmission in the strip-shaped network, where the length is significantly greater than the width. While the spatial pipelining always hurts the throughput in the disk networks with the free-space path loss $\alpha = 2$, in the strip networks it is feasible to improve the network throughput by spatial pipelining regardless of the path attenuation with $\alpha \geq 2$, which is proven by theoretical analysis. Moreover, we show the distinct propagation properties of the spatially pipelined OLA transmission, and use the properties to build a simplified multi-packet propagation model with a fixed step-size for the throughput optimization process that reduces the exhaustive search range. The numerical results show the impacts of the different system parameters on the optimal throughput in the finite network. Potential extensions of this paper include addressing a wider scenario with low diversity orders and low node densities.

APPENDIX

The properties in Section II-C2 with $\alpha > 2$ are proved as follows. The proof procedure is the same as [10], which assumes $\alpha = 2$, but the following functions and equations corresponding to $\alpha > 2$ are different from [10].

1) When $f(y) := \int_y^{y+x} G(u, \alpha, W)du$ with G is the term inside the integral in (6), $f(y)$ is a monotonically decreasing function with respect to y, because the derivative of $f(\cdot)$ is given by

$$f'(y) = G(y + x, \alpha, W) - G(y, \alpha, W). \tag{21}$$

For positive $\overline{P}_r$ and W with $\alpha > 2$, it can be seen that $f'(y) < 0$ by inspection. Also, the limiting values at zero and infinity can be found as $\lim_{y\to 0} f(y) = \infty$ and $\lim_{y\to\infty} f(y) = 0$. Hence, there always exists a unique solution of the equation $f(y) = \tau$.

2) When $\int_{h(x)}^{h(x)+x} G(u, \alpha, W)du = \frac{\tau}{\overline{P}_r}$, $h'(x)$ can be obtained by differentiating the both sides with respect to x as

$$h'(x) = \frac{G(h(x) + x, \alpha, W)}{G(h(x), \alpha, W) - G(h(x) + x, \alpha, W)}, \tag{22}$$

The derivative of $G(x, \alpha, \overline{P}_r, W)$ with respect to x is given by

$$\begin{aligned}
\frac{dG(x,\alpha,W)}{dx} &= \frac{1}{8(\alpha-2)Wx^5}\left(\frac{W^2}{4} + x^2\right)^{-\alpha/2} \\
&\times \Big(4W^4x^2\Upsilon_1 + 8\alpha W^2x^4\Upsilon_1 - 64x^6\Upsilon_1 + 32\alpha x^6\Upsilon_1 \\
&- 20W^4x^2\Upsilon_2 + 4\alpha W^4x^2\Upsilon_2 - 40\alpha W^2x^4\Upsilon_2 + 8\alpha^2W^2x^4\Upsilon_2 \\
&+ 64x^6\Upsilon_2 - 32\alpha x^6\Upsilon_2 + 3W^6\Upsilon_3 - \alpha W^6\Upsilon_3 + 24W^4x^2\Upsilon_3 \\
&- 8\alpha W^4x^2\Upsilon_3 + 48W^2x^4\Upsilon_3 - 16\alpha W^2x^4\Upsilon_3 + 15W^6\Upsilon_4 \\
&- 8\alpha W^6\Upsilon_4 + \alpha^2W^6\Upsilon_4 + 72W^4x^2\Upsilon_4 - 36\alpha W^4x^2\Upsilon_4 \\
&+ 4\alpha^2W^4x^2\Upsilon_4 + 48W^2x^4\Upsilon_4 - 16\alpha W^2x^4\Upsilon_4\Big),
\end{aligned} \tag{23}$$

where $\Upsilon_1 = {}_2F_1\big(1, \frac{3-\alpha}{2}, \frac{-1}{2}, \frac{-W^2}{4x^2}\big)$, $\Upsilon_2 = {}_2F_1\big(1, \frac{3-\alpha}{2}, \frac{1}{2}, \frac{-W^2}{4x^2}\big)$, $\Upsilon_3 = {}_2F_1\big(2, 1 + \frac{3-\alpha}{2}, \frac{1}{2}, \frac{-W^2}{4x^2}\big)$, and $\Upsilon_4 = {}_2F_1\big(2, 1 + \frac{3-\alpha}{2}, \frac{3}{2}, \frac{-W^2}{4x^2}\big)$. Because $\frac{dG(x,\alpha,W)}{dx} < 0$ for $x > 0$, $G(x, \alpha, W)$ is a monotonically decreasing function with respect to x. Therefore, $h'(x)$ is always positive for $x > 0$, which means $h(\cdot)$ is monotonically increasing.

3) If we denote $G(x, \alpha, W)$ by $G(x)$ in short and $\frac{dG(x,\alpha,W)}{dx}$ by $G'(x)$, the second derivative of $h(\cdot)$ with respect to x is given by

$$h''(x) = \frac{(h'+1)G'(h+x)G(h) - G(h+x)G'(h)h'}{(G(h) - G(h+x))^2}. \tag{24}$$

To show the concavity (i.e., $h''(x) < 0$), the numerator should be negative, which means $(h'+1)G'(h+x)G(h) < G(h+x)G'(h)h'$. By dividing the both sides by h', which is positive as proven in the second property, the inequality is given by $(h'+1)G'(h+x)G(h)/h' < G(h+x)G'(h)$. If plugging (22), it can be expressed as

$$\frac{-G'(h+x)}{(G(h+x))^2} > \frac{-G'(h)}{(G(h))^2}, \tag{25}$$

It is true, because $\frac{-G'(h)}{(G(h))^2}$ is increasing for any positive $\alpha, W, \overline{P}_r$, which is given by

$$\begin{aligned}
&\frac{-G'(h)}{(G(h))^2} = 2(2-\alpha)W\big(\frac{W^2}{4} + x^2\big)^{\alpha/2}\Big(4W^4x^2\Upsilon_1 \\
&+ 8\alpha W^2x^4\Upsilon_1 - 64x^6\Upsilon_1 + 32\alpha x^6\Upsilon_1 - 20W^4x^2\Upsilon_2 \\
&+ 4\alpha W^4x^2\Upsilon_2 - 40\alpha W^2x^4\Upsilon_2 + 8\alpha^2W^2x^4\Upsilon_2 + 64x^6\Upsilon_2 \\
&- 32\alpha x^6\Upsilon_2 + 3W^6\Upsilon_3 - \alpha W^6\Upsilon_3 + 24W^4x^2\Upsilon_3 \\
&- 8\alpha W^4x^2\Upsilon_3 + 48W^2x^4\Upsilon_3 - 16\alpha W^2x^4\Upsilon_3 + 15W^6\Upsilon_4 \\
&- 8\alpha W^6\Upsilon_4 + \alpha^2W^6\Upsilon_4 + 72W^4x^2\Upsilon_4 - 36\alpha W^4x^2\Upsilon_4 \\
&+ 4\alpha^2W^4x^2\Upsilon_4 + 48W^2x^4\Upsilon_4 - 16\alpha W^2x^4\Upsilon_4\Big) \\
&/\Big(x\big(W^2 + 4x^2\big)^2\big(W^2\Upsilon_1 + 4x^2\Upsilon_1 - 5W^2\Upsilon_2 + \alpha W^2\Upsilon_2 \\
&- 4x^2\Upsilon_2\big)^2\Big).
\end{aligned} \tag{26}$$

Hence, $h(\cdot)$ is concave.

REFERENCES

[1] J. Laneman, D. Tse, and G. Wornell, "Cooperative diversity in wireless networks: efficient protocols and outage behavior," *IEEE Trans. Inf. Theory*, vol. 50, no. 12, pp. 3062–3080, Dec. 2004.

[2] A. Scaglione and Y.-W. Hong, "Opportunistic large arrays: cooperative transmission in wireless multihop ad hoc networks to reach far distances," *IEEE Trans. Signal Process.*, vol. 51, no. 8, pp. 2082–2092, Aug. 2003.

[3] I. Maric and R. Yates, "Cooperative multihop broadcast for wireless networks," *IEEE J. Sel. Areas Commun.*, vol. 22, no. 6, pp. 1080–1088, Aug. 2004.

[4] G. Jakllari, S. V. Krishnamurthy, M. Faloutsos, and P. V. Krishnamurthy, "On broadcasting with cooperative diversity in multi-hop wireless networks," *IEEE J. Sel. Areas Commun.*, vol. 25, no. 2, pp. 484–496, Feb. 2007.

[5] T. Halford and K. Chugg, "Barrage relay networks," in *Proc. 2010 Inf. Theory Applications Workshop*, pp. 1–8.

[6] Y. J. Chang, H. Jung, and M. A. Ingram, "Demonstration of an OLA-based cooperative routing protocol in an indoor environment," in *Proc. 2011 IEEE European Wireless*, pp. 1–8.

[7] L. Thanayankizil, A. Kailas, and M. A. Ingram, "Routing for wireless sensor networks with an opportunistic large array (OLA) physical layer," *Ad Hoc Sensor Wireless Netw.*, vol. 8, no. 1-2, pp. 79–117, 2009.

[8] B. Sirkeci-Mergen, A. Scaglione, and G. Mergen, "Asymptotic analysis of multistage cooperative broadcast in wireless networks," *IEEE Trans. Inf. Theory*, vol. 52, no. 6, pp. 2531–2550, June 2006, corrected version. Available: http://crisp.ece.cornell.edu/papers/BirsenITTran2006.pdf.

[9] A. Kailas and M. A. Ingram, "Alternating opportunistic large arrays in broadcasting for network lifetime extension," *IEEE Trans. Wireless Commun.*, vol. 8, no. 6, pp. 2831–2835, 2009.

[10] B. Sirkeci-Mersen and A. Scaglione, "A continuum approach to dense wireless networks with cooperation," in *Proc. 2005 INFOCOM*, vol. 4, pp. 2755–2763.

[11] A. Kailas and M. A. Ingram, "Analysis of a simple recruiting method for cooperative routes and strip networks," *IEEE Trans. Wireless Commun.*, vol. 9, no. 8, pp. 2415–2419, Aug. 2010.

[12] S. Hassan and M. A. Ingram, "A quasi-stationary markov chain model of a cooperative multi-hop linear network," *IEEE Trans. Wireless Commun.*, vol. 10, no. 7, pp. 2306–2315, 2011.

[13] ——, "On the modeling of randomized distributed cooperation for linear multi-hop networks," in *Proc. 2012 IEEE ICC*, pp. 366–370.

[14] T. Halford, K. Chugg, and A. Polydoros, "Barrage relay networks: system and protocol design," in *Proc. 2010 IEEE PIMRC*, pp. 1133–1138.

[15] C. E. Perkins, E. M. Belding-Royer, and S. R. Das, "Ad hoc on-demand distance vector (AODV) routing," published online, Internet Engineering Task Force, RFC Experimental 3561, July 2003.

[16] W. Ge, J. Zhang, and G. Xue, "Cooperative geographic routing in wireless sensor networks," in *Proc. 2006 IEEE MILCOM*, pp. 1–7.

[17] S. Kim, S. Pakzad, D. Culler, J. Demmel, G. Fenves, S. Glaser, and M. Turon, "Health monitoring of civil infrastructures using wireless sensor networks," in *Proc. 2007 IEEE Intl Symp. Inf. Process. Sensor Netw.*, pp. 254–263.

[18] D. De Caneva, P. Montessoro, and D. Pierattoni, "WiWi: deterministic and fault tolerant wireless communication over a strip of pervasive devices," in *Proc. 2008 IEEE Wireless Commun., Netw., Mobile Comput. Conf.*, pp. 1–5.
[19] B. Sirkeci-Mergen and M. Gastpar, "On the broadcast capacity of wireless networks with cooperative relays," *IEEE Trans. Inf. Theory*, vol. 56, no. 8, pp. 3847–3861, Aug. 2010.
[20] M.-K. Oh, X. Ma, G. Giannakis, and D.-J. Park, "Cooperative synchronization and channel estimation in wireless sensor networks," in *Proc. 2003 IEEE Conf. Signals, Syst. Comput.*, vol. 1, pp. 238–242.
[21] H. Jung and M. A. Ingram, "Analysis of spatial pipelining in opportunistic large array broadcasts," in *Proc. 2011 IEEE MILCOM*, pp. 991–996.
[22] H. Jung and M. A. Weitanuer, "Multi-packet interference in opportunistic large array broadcasts over disk networks," *IEEE Trans. Wireless Commun.*, vol. PP, no. 99, pp. 1–15, 2013.
[23] H. Jung and M. A. Ingram, "Analysis of intra-flow interference in opportunistic large array transmission for strip networks," in *Proc. 2012 IEEE ICC*.
[24] G. Jakllari, S. V. Krishnamurthy, M. Faloutsos, P. V. Krishnamurthy, and O. Ercetin, "A cross-layer framework for exploiting virtual MISO links in mobile ad hoc networks," *IEEE Trans. Mobile Comput.*, vol. 6, no. 6, pp. 579–594, June 2007.
[25] S. Lakshmanan and R. Sivakumar, "Diversity routing for multi-hop wireless networks with cooperative transmissions," in *Proc. 2009 IEEE SECON*, pp. 1–9.
[26] J. W. Jung and M. A. Ingram, "Residual-energy activated cooperative transmission (REACT) to avoid the energy hole," in *Proc. 2010 IEEE ICC*.
[27] B. Bash, D. Goeckel, and D. Towsley, "Clustering in cooperative networks," in *Proc. 2011 IEEE INFOCOM*, pp. 486–490.
[28] H. Jung and M. A. Ingram, "SNR penalty from the path-loss disparity in virtual multiple-input-single-output (VMISO) link," in *Proc. 2013 IEEE ICC*.
[29] G. L. Stuber, *Principles of Mobile Communications*, 2nd ed. Kluwer Academics Publishers, 2000.
[30] A. Kailas, L. Thanayankizil, and M. A. Ingram, "A simple cooperative transmission protocol for energy-efficient broadcasting over multi-hop wireless networks," *J. Commun. Netw.*, vol. 10, no. 2, pp. 213–220, 2008.
[31] M. Abramowitz and I. Stegun, *Handbook of Mathematical Functions with Formulas, Graphs, and Mathematical Tables*. Dover Publications, 1964, vol. 55, no. 1972.
[32] A. Bader and E. Ekici, "Performance optimization of interference-limited multihop networks," *IEEE/ACM Trans. Netw.*, vol. 16, no. 5, pp. 1147–1160, Oct. 2008.
[33] M. Garetto, T. Salonidis, and E. Knightly, "Modeling per-flow throughput and capturing starvation in CSMA multi-hop wireless networks," *IEEE/ACM Trans. Netw.*, vol. 16, no. 4, pp. 864–877, Aug. 2008.
[34] Y. J. Chang, M. A. Ingram, and S. Frazier, "Cluster transmission time synchronization for cooperative transmission using software defined radio," in *Proc. 2010 IEEE ICC*.
[35] J. Proakis, *Digital Communications*. McGraw-Hill, 2000.
[36] R. Ramanathan, "Challenges: a radically new architecture for next generation mobile ad hoc networks," in *Proc. ACM MobiCom*.
[37] H. Jung and M. A. Weitnauer, "Link asymmetry in virtual miso-based networks," to be presented at *2013 IEEE MILCOM*.
[38] T. Rappaport, *Wireless Communications: Principles and Practice*. Prentice Hall PTR, 2001.

Haejoon Jung received the B.S. degree from Yonsei University, Seoul, South Korea in 2008. He is currently pursuing his Ph.D. degree in Electrical and Computer Engineering at the Georgia Institute of Technology (Georgia Tech), Atlanta, USA. He has been working in the Smart Antenna Research Laboratory (SARL) as a graduate research assistant. His research interests include wireless network and communication system, focusing on cooperative communications. He also worked for Samsung Electronics (Kihueng, South Korea) as a summer intern in 2009 and 2011.

Mary Ann Weitnauer (formerly Mary Ann Ingram) received the B.E.E. and Ph.D. degrees from the Georgia Institute of Technology (Georgia Tech), Atlanta, USA, in 1983 and 1989, respectively. In 1989, she joined the faculty of the School of Electrical and Computer Engineering at Georgia Tech, where she is currently Professor. Her early research areas were optical communications and radar systems. In 1997, she established the Smart Antenna Research Laboratory (SARL) at Georgia Tech, which applies real and virtual array antennas to wireless networks and radar systems. She held the Georgia Tech ADVANCE Professorship for the College of Engineering from 2006-2012. She was a Visiting Professor at Aalborg University, Aalborg, Denmark in the summers of 2006-2008 and at Idaho National Labs in 2010. The SARL performs system analysis and design, channel measurement, and prototyping relating primarily to wireless local area, ad hoc and sensor networks, with focus on the lower three layers of the protocol stack. SARL has also recently developed signal processing algorithms for impulse radio ultrawideband (IR-UWB) for non-contact vital signs measurement. Dr. Weitnauer has authored or co-authored over 160 refereed journal and conference papers, including four conference papers that have won "Best Paper" awards. She served as a Guest Editor for the EURASIP Special Issue on Cross-Layered Design for Physical/MAC/Link layers in Wireless Systems in 2007 and Co-Chair for America for the IEEE Wireless VITAE Conference in 2009. She was an associate editor for the IEEE TRANSACTIONS ON MOBILE COMPUTING from 2009-2012. Dr. Weitnauer is a Senior Member of the IEEE.